Scattering from an impedance cylinder embedded in a nonconcentric dielectric cylinder

R.P. Parrikar, MSc
A.A. Kishk, PhD
A.Z. Elsherbeni, PhD

Indexing terms: Electromagnetic theory, Radar and radionavigation

Abstract: The electromagnetic scattering from an impedance cylinder embedded in a nonconcentric dielectric cylinder is derived rigorously by using a boundary value approach. The two cylinders are assumed to be infinite in length and of circular cross-section. The incident electromagnetic field is in terms of an electric or a magnetic field component parallel to both cylinder axes. The problem is two dimensional and the solution to either types of polarisation (TM or TE) can be found independently. Plane wave and line source excitations are considered in this analysis. The effects of various geometrical and electrical parameters (such as the cylinder's radii, permittivity, surface impedance and eccentricity) on the near field distribution and the far scattered field pattern are examined. Bistatic and monostatic scattering cross-sections of the composite cylinder which minimise or maximise the radar cross-section are also investigated.

1 Introduction

Scattering from concentric dielectric loaded cylinders have been studied by a number of researchers using different techniques [1–7], whereas work on the eccentric geometry has been less extensive. The motivation for considering analytical and exact solutions to such problems arises from their usefulness in the detection of conducting objects embedded in dielectrics, in the determination of scattering by impurities in dielectric structures and in the enhancement of antenna directivity with an eccentric coating [8]. Scattering data from complex bodies is often used to obtain information about their internal structure such as inhomogenities and nonsymmetries. The eccentric coating of scattering objects may also have pronounced effects on the increase or decrease of its scattering cross-section. Other applications are in the biomedical area [9–10] and in the modelling of forests for remote sensing. The scattering from eccentric cylinders and spheres has been investigated by Roumeliotis *et al.* [11–13] and the theory of the circular waveguide with an eccentric metallic conductor has been developed by Veselov and Semenov [14]. Roumeliotis and Fikioris have also pursued the eccentric waveguide problem in detail [15].

Paper 7844H (E11), first received 6th March and in revised form 19th September 1990

The authors are with the Electrical Engineering Department, University of Mississippi, Mississippi 38677, USA

The present paper deals with the scattering characteristics of an imperfectly conducting cylinder in an eccentric dielectric coating. The usual procedure is similar to that of Reference 14, the present treatment is much more general. In Reference 14, the small argument approximation of the Bessel functions has been used to obtain simple expressions for the scattering cross-section of an eccentric dielectric loaded conducting cylinder due to an incident plane wave. However, such an approximation only gives accurate results for small values of eccentricity. The present analysis does not suffer from this limitation. Also, the dielectric coating losses have been accounted for by allowing the dielectric constants to be complex and the incident field is from a line source. The plane wave field is a special case; when the line source recedes to infinity. The problem is solved for TM to z polarised wave and it is shown subsequently how the solution to the corresponding TE to z polarisation can be easily obtained. The field expressions in the dielectric region and in the outside free space region are expressed in terms of sets of cylindrical harmonic functions with unknown expansion coefficients. To find the unknown coefficients, the addition theorem of cylindrical functions is used to transform the field components between the local co-ordinates of the two cylinders. The continuity of the tangential electric and magnetic field components on the surfaces of the two cylinders is then enforced. As a result, a set of infinite equations is obtained which is transformed into matrix form and then solved numerically after proper truncation. The validity of the solution is verified by comparing the numerical results of special cases with those based on other well known exact solutions.

2 Formulation

Consider a TM to z wave illuminating a composite cylinder, as shown in Fig. 1. The inner cylinder of radius a is an imperfect conductor characterised by a surface impedance η_s which is coated by a dielectric cylinder of radius b. The dielectric material is linear, homogeneous, isotropic and characterised by constants ε_{r1} and μ_{r1} or equivalently by the intrinsic wave impedance η_1. The distance between the axes of the two cylinders, called the eccentricity, is denoted e and the composite arrangement is immersed in free space which is characterised by ε_0 and μ_0 or η_0. The incident electric field from an infinite electric line current located at (ρ_0, ϕ_0) and parallel to the z axis of a cylindrical co-ordinate system is given by

$$E_z^{il}(\rho, \phi) = E_0^l H_0^{(2)}(k_0 |\bar{\rho} - \bar{\rho}_0|) \tag{1}$$

where

$$E_0^l = -\frac{\eta_0 k_0 I}{4} \tag{2}$$

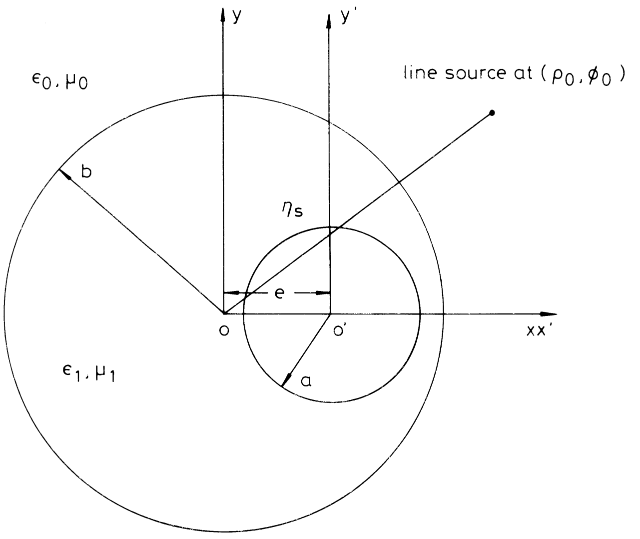

Fig. 1 *Problem geometry*

I is the strength of the current filament and $k_0(2\pi/\lambda_0)$ is the wave number in free space. E_z^{il} is given in terms of a series expansion, i.e.

$$E_z^{il} = \begin{cases} E_0^l \sum_{n=-\infty}^{\infty} H_n^{(2)}(k_0 \rho_0) J_n(k_0 \rho) e^{jn(\phi - \phi_0)} & \rho < \rho_0 \\ E_0^l \sum_{n=-\infty}^{\infty} H_n^{(2)}(k_0 \rho) J_n(k_0 \rho_0) e^{jn(\phi - \phi_0)} & \rho > \rho_0 \end{cases} \tag{3}$$

where J_n and H_n are the Bessel function of the first kind and Hankel function of the second kind, respectively. The time dependence $e^{j\omega t}$ is tacitly assumed. The superscripts i and l represent the incident and line source type of excitation, respectively. The z component of the total electric field in free space region is expressed with respect to the $x0y$ reference frame as follows:

$$E_z^f(\rho, \phi) = E_0^l \sum_{n=-\infty}^{\infty} [H_n^{(2)}(k_0 \rho_0) J_n(k_0 \rho) + a_n H_n^{(2)}(k_0 \rho)] e^{jn(\phi - \phi_0)} \quad \rho < \rho_0 \tag{4}$$

The electric field in the dielectric region with respect to the $x'0'y'$ reference frame is

$$E_z^d(\rho', \phi') = E_0^l \sum_{n=-\infty}^{\infty} [b_n J_n(k_1 \rho') + c_n H_n^{(2)}(k_1 \rho')] e^{jn\phi'} \tag{5}$$

where a_n, b_n and c_n are the unknown coefficients and k_1 is the wave number in the dielectric region. Therefore, the ϕ component of the magnetic field in the dielectric region is given by

$$H_\phi^d(\rho', \phi') = \frac{E_0^l}{j\eta_1} \sum_{n=-\infty}^{\infty} [b_n J_n'(k_1 \rho') + c_n H_n^{(2)\prime}(k_1 \rho')] e^{jn\phi'} \tag{6}$$

where primes denote derivatives with respect to the arguments. The impedance boundary condition [16] at $\rho' = a$ is

$$E_z^d(a, \phi') = \eta_s H_\phi^d(a, \phi') \tag{7}$$

which leads to

$$\sum_{m=-\infty}^{\infty} [b_n J_n(k_1 a) + c_n H_n^{(2)}(k_1 a)] e^{jn\phi'} = -j \frac{\eta_s}{\eta_1} \sum_{n=-\infty}^{\infty} [b_n J_n'(k_1 a) + c_n H_n^{(2)\prime}(k_1 a)] e^{jn\phi'} \tag{8}$$

Multiplying eqn. 8 by $e^{jl\phi'}$ and integrating with respect to ϕ from 0 to 2π, gives

$$c_l = T_l b_l \tag{9}$$

where

$$T_l = -\frac{\eta_1 J_l(k_1 a) + j\eta_s J_l'(k_1 a)}{\eta_1 H_l^{(2)}(k_1 a) + j\eta_s H_l^{(2)\prime}(k_1 a)} \tag{10}$$

To apply the boundary conditions at $\rho = b$, $E^d(\rho', \phi')$ has to be referred to the $x0y$ co-ordinate system. This is possible using the addition theorem for cylindrical Bessel and Hankel functions [17], i.e.

$$B_n(k\rho') e^{jn\phi'} = \begin{cases} \sum_{m=-\infty}^{\infty} B_{m-n}(ke) J_m(k\rho) e^{jm\phi} & \rho < e \\ \sum_{m=-\infty}^{\infty} J_{m-n}(ke) B_m(k\rho) e^{jm\phi} & \rho > e \end{cases} \tag{11}$$

where $B_n(x)$ is a Bessel function or a Hankel function of order n and argument x. Applying the above addition theorem to eqn. 5 results in

$$E_z^d(\rho, \phi) = E_0^l \sum_{n=-\infty}^{\infty} \sum_{m=-\infty}^{\infty} J_{m-n}(k_1 e) \times [b_n J_m(k_1 \rho) + c_n H_m^{(2)}(k_1 \rho)] e^{jm\phi} \tag{12}$$

The second term on the right hand side of eqn. 12 has been translated for $\rho > e$. This is because the application of the boundary condition at $\rho = b$ implies that $\rho > e$. The continuity of the tangential electric field component at $\rho = b$ yields

$$\sum_{n=-\infty}^{\infty} [H_n^{(2)}(k_0 \rho_0) J_n(k_0 b) + a_n H_n^{(2)}(k_0 b)] e^{jn(\phi - \phi_0)} = \sum_{n=-\infty}^{\infty} \sum_{m=-\infty}^{\infty} J_{m-n}(k_1 e) \times [b_n J_m(k_1 b) + c_n H_n^{(2)}(k_1 b)] e^{jm\phi} \tag{13}$$

The orthogonality of the exponential functions in eqn. 13 is now used to extract a_l, *viz*

$$a_l = \frac{1}{H_l^{(2)}(k_0 b)} \left(-H_l^{(2)}(k_0 \rho_0) J_l(k_0 b) + e^{jl\phi_0} \sum_{n=-\infty}^{\infty} J_{l-n}(k_1 e) [b_n J_l(k_1 b) + c_n H_l^{(2)}(k_1 b)] \right) \tag{14}$$

The ϕ component of the magnetic field in free space and dielectric regions referred to the $x0y$ co-ordinate system is, respectively,

$$H_\phi^f(\rho, \phi) = \frac{E_0^l}{j\eta_0} \sum_{n=-\infty}^{\infty} [H_n^{(2)}(k_0 \rho_0) J_n'(k_0 \rho) + a_n H_n^{(2)\prime}(k_0 \rho)] e^{jn(\phi - \phi_0)} \tag{15}$$

$$H_\phi^d(\rho, \phi) = \frac{E_0^l}{j\eta_1} \sum_{n=-\infty}^{\infty} \sum_{m=-\infty}^{\infty} J_{m-n}(k_1 e) \times [b_n J_m'(k_1 \rho) + c_n H_m^{(2)\prime}(k_1 \rho)] e^{jm\phi} \tag{16}$$

The continuity of the above H_ϕ components at $\rho = b$ together with the orthogonality of exponential functions results in

$$a_l = \frac{1}{H_l^{(2)'}(k_0 b)} \left(-H_l^{(2)}(k_0 \rho_0) J_l'(k_0 b) + \frac{\eta_0}{\eta_1} e^{jl\phi_0} \times \sum_{n=-\infty}^{\infty} J_{l-n}(k_1 e)[b_n J_l'(k_1 b) + c_n H_l^{(2)'}(k_1 b)] \right) \quad (17)$$

Combining eqn. 9 with eqns. 14 and 17, an expression solely in terms of b_n is obtained, i.e.

$$\sum_{n=-\infty}^{\infty} F_{ln} b_n = D_l \quad (18)$$

where

$$F_{ln} = \frac{e^{jl\phi_0}}{H_l^{(2)}(k_0 \rho_0)} J_{l-n}(k_1 e) \left(J_l(k_1 b) + T_n H_l^{(2)}(k_1 b) - \frac{\eta_0 H_l^{(2)}(k_0 b)}{\eta_1 H_l^{(2)'}(k_0 b)} [J_l'(k_1 b) + T_n H_l^{(2)'}(k_1 b)] \right) \quad (19)$$

$$D_l = \frac{2}{j\pi k_0 b H_l^{(2)'}(k_0 b)} \quad (20)$$

Eqn. 18 represents a set of infinite equations which is transformed into matrix form and then solved numerically after proper truncation to retrieve the unknown coefficient b_n. The remaining unknown coefficients, c_n and a_n, are evaluated using eqns 9 and 14 or 17, respectively. Plane wave excitation is obtained by letting the line source recede to infinity. The electric field component of the incident plane wave is then given by

$$E_z^{ip}(\rho, \phi) = E_0^p e^{jk\rho \cos(\phi - \phi_0)} \quad (21)$$

where

$$E_0^p = E_0^l \sqrt{\left(\frac{2i}{\pi k \rho_0}\right)} e^{-jk\rho_0} \quad (22)$$

and the incident angle ϕ_0 is measured in the anticlockwise direction from the positive x axis. The field expressions for the case of plane wave excitation are obtained by simply replacing $H_l^{(2)}(k_0 \rho_0)$ by j^l in eqns. 14, 17 and 19.

The scattered electric field in free space is given by

$$E_z^s(\rho, \phi) = E_0^g \sum_{n=-\infty}^{\infty} a_n H_n^{(2)}(k_0 \rho) e^{jn(\phi - \phi_0)} \quad (23)$$

where the superscript g is equal to p or l for plane wave or line source incident field, respectively. The far scattered field pattern is determined after using the large argument approximation of the Hankel function and normalising the resulting expression by the factor $E_0^g \sqrt{[2j/(\pi k \rho)]} e^{-jk\rho}$. Thus the scattered field pattern $F^{sg}(\phi, \phi_0)$ reduces to

$$F^{sg}(\phi, \phi_0) = \sum_{n=-\infty}^{\infty} a_n j^n e^{jn(\phi - \phi_0)} \quad (24)$$

The properties of a plane wave scattered by cylindrical objects of infinite length along one of the co-ordinate axes are usually described in terms of the scattering cross-section which is denoted by σ and defined as

$$\sigma(\phi) = \lim_{\rho \to \infty} 2\pi\rho \left| \frac{E_z^{sp}(\rho, \phi, \phi_0)}{E_z^{ip}} \right|^2 \quad (25)$$

where E_z^{sp} and E_z^{ip} are the scattered and incident z components of the electric field. The scattering cross-section of the composite cylinder is then given by

$$\sigma(\phi) = \frac{2}{\pi} |F^{sp}(\phi, \phi_0)|^2 \quad (26)$$

The solution of the same problem due to an incident field from an infinite magnetic line current parallel to the z axis or from a plane wave with a magnetic field component parallel to the z axis (TE excitation) is straightforward and similar to the foregoing analysis. However, application of the duality principle [18], yields the unknown coefficients for the TE case by replacing η_i by $1/\eta_i$ in eqns. 10 and 19, where i denotes 0 for the free space region, 1 for the dielectric region or s for the inner cylinder surface impedance.

3 Numerical results and discussion

The expressions developed above can easily be specialised to simple geometries such as a perfectly conducting cylinder in free space. By setting $\varepsilon_1 = \varepsilon_0$ and $\eta_s = 0$, an exact expression for the scattered field from a perfectly conducting cylinder in free space, similar to the one in standard textbooks, can be obtained after some mathematical manipulation. For such a case, the analytical expression for the unknown coefficient b_l is reduced to

$$b_l = \begin{cases} H_l^{(2)}(k_0 \rho_0) e^{jl\phi_0} & \text{line source excitation} \\ j^l e^{jl\phi_0} & \text{plane wave excitation} \end{cases} \quad (27)$$

which then yields the following expression for the unknown scattering coefficient a_l

$$a_l = \begin{cases} -H_l^{(2)}(k_0 \rho_0) \dfrac{J_l(k_0 a)}{H_l^{(2)}(k_0 a)} & \text{line source excitation} \\ -j^l \dfrac{J_l(k_0 a)}{H_l^{(2)}(k_0 a)} & \text{plane wave excitation} \end{cases} \quad (28)$$

The exact expression for a dielectric coated concentric conducting cylinder can also be obtained in a fairly straightforward manner.

The above analysis has been implemented in a Fortran program from which sample numerical results are presented in the following sections and the values of η_s are normalised to η_0.

Table 1 lists some values of the forward and back scattering cross-sections (σ_f and σ_b, respectively) as a function of the integer k which is the absolute value of the upper limit of the index of summation in the series

Table 1: Scattering cross-section against k for $a = 0.3\lambda$, $b = 0.5\lambda$, $e = 0.2\lambda$, $\varepsilon_{r1} = 4.37 - j0.16$, $\eta_s = 0.5 - j0.5$ and $\phi_0 = 180°$

	TM polarisation		TE polarisation	
K	σ_f	σ_b	σ_f	σ_b
1	1.736381	0.844243	1.361709	0.766243
2	5.902783	0.883719	2.440005	0.868401
3	7.651909	0.241823	6.358829	0.152940
4	9.181424	0.288197	7.966280	0.287813
5	9.755219	0.280164	8.662320	0.243955
6	9.882924	0.270770	8.572824	0.250221
7	9.860407	0.272214	8.575802	0.249465
8	9.861811	0.272097	8.575277	0.249482
9	9.861092	0.272112	8.575312	0.249479
10	9.861053	0.272114	8.575312	0.249479
11	9.861019	0.272114	8.575331	0.249480
12	9.861019	0.272114	8.575321	0.249480
13	9.861019	0.272114	8.575331	0.249480
14	9.861010	0.272114	8.575321	0.249480

expressions. It is clear that not many terms yield a convergent solution for both TE and TM excitation.

Figs. 2 and 3 display σ_f as a function of ϕ_0 for an incident TM polarised wave on a coated, perfectly conducting and capacitive cores, respectively. In the former case, σ_f for $e = 0.1\lambda_0$ and $0.2\lambda_0$ stays well below the corresponding values for $e = 0$ and in the latter case, σ_f exhibits the opposite behaviour. The parameters in Figs. 4 and 5 are similar to those in Figs. 2 and 3 but for a TE polarised wave. With a capacitive core (Fig. 5), σ_f for $e = 0.1\lambda_0$ and $0.2\lambda_0$ is always less than that for $e = 0$ but this is not always the case with a perfectly conducting core as shown in Fig. 4.

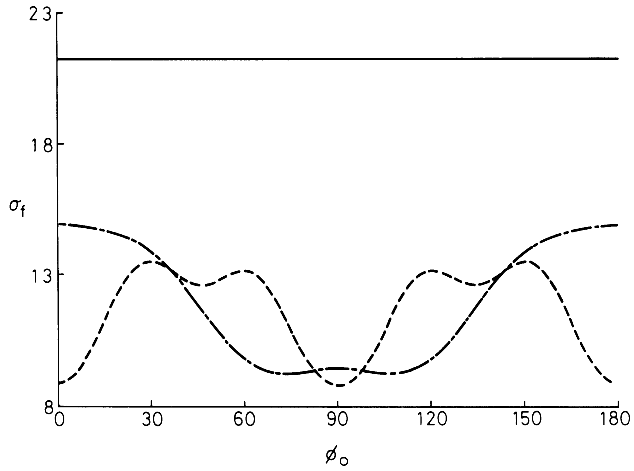

Fig. 2 *σ_f against ϕ_0 with $a = 0.3\lambda_0$, $b = 0.5\lambda_0$, $\varepsilon_{r1} = 4.37 - j0.16$ and $\eta_s = 0$ (TM polarisation)*
—— $e = 0$ — — — $e = 0.1\lambda_0$ - - - - $e = 0.2\lambda_0$

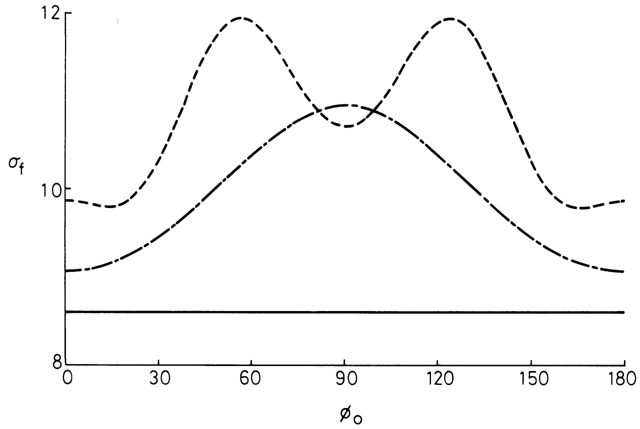

Fig. 3 *σ_f against ϕ_0 with $a = 0.3\lambda_0$, $b = 0.5\lambda_0$, $\varepsilon_{r1} = 4.37 - j0.16$ and $\eta_s = 0.5 - j0.5$ (TM polarisation)*
—— $e = 0$ — — — $e = 0.1\lambda_0$ - - - - $e = 0.2\lambda_0$

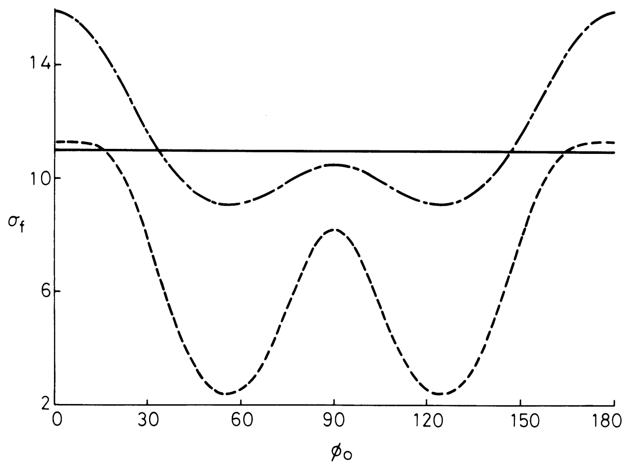

Fig. 4 *σ_f against ϕ_0 with $a = 0.3\lambda_0$, $b = 0.5\lambda_0$, $\varepsilon_{r1} = 4.37 - j0.16$ and $\eta_s = 0$ (TE polarisation)*
—— $e = 0$ — — — $e = 0.1\lambda_0$ - - - - $e = 0.2\lambda_0$

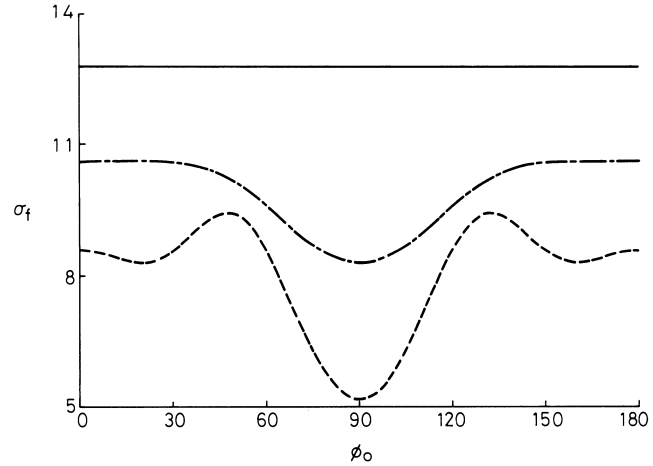

Fig. 5 *σ_f against ϕ_0 with $a = 0.3\lambda_0$, $b = 0.5\lambda_0$, $\varepsilon_{r1} = 4.37 - j0.16$ and $\eta_s = 0.5 - j0.5$ (TE polarisation)*
—— $e = 0$ — — — $e = 0.1\lambda_0$ - - - - $e = 0.2\lambda_0$

Figs. 6 and 7 display σ_b with $e = 0.2\lambda_0$ for different values of η_s. As η_s approaches the intrinsic impedance of the dielectric coating ($\simeq 0.478\eta_0$), σ_b tends to 'flatten out'. This may be because of an impedance matching between the core and the coating material.

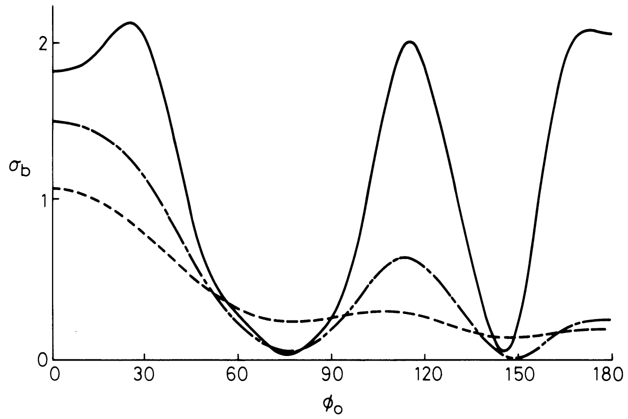

Fig. 6 *σ_b against ϕ_0 with $a = 0.3\lambda_0$, $b = 0.5\lambda_0$, $e = 0.2\lambda_0$, and $\varepsilon_{r1} = 4.37 - j0.16$ (TM polarisation)*
—— $\eta_s = 0$ — — — $\eta_s = 0.2$ - - - - $\eta_s = 0.4$

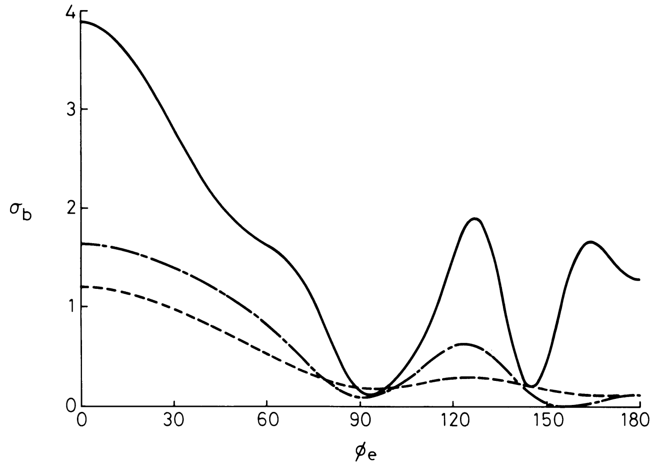

Fig. 7 *σ_b against ϕ_0 with $a = 0.3\lambda_0$, $b = 0.5\lambda_0$, $e = 0.2\lambda_0$, and $\varepsilon_{r1} = 4.37 - j0.16$ (TE polarisation)*
—— $\eta_s = 0$ — — — $\eta_s = 0.2$ - - - - $\eta_s = 0.4$

Figs. 8 and 9 show σ_f against the real part of $\varepsilon_{r1}(\varepsilon_r)$ for $\eta_s = 0$ and $0.5 - j0.5$, respectively, for an incident TM plane wave with $\phi_0 = 180°$, $a = 0.3\lambda_0$, $b = 0.5\lambda_0$ and the imaginary part of ε_{r1} equal to -0.16. The corresponding curves of σ_b against ε_r are also shown in Figs. 10 and 11. Sharp values for σ_f are observed (Fig. 8) when the core is perfectly conducting, however for an impedance core (Fig. 9), the variations in σ_f are relatively smoother and

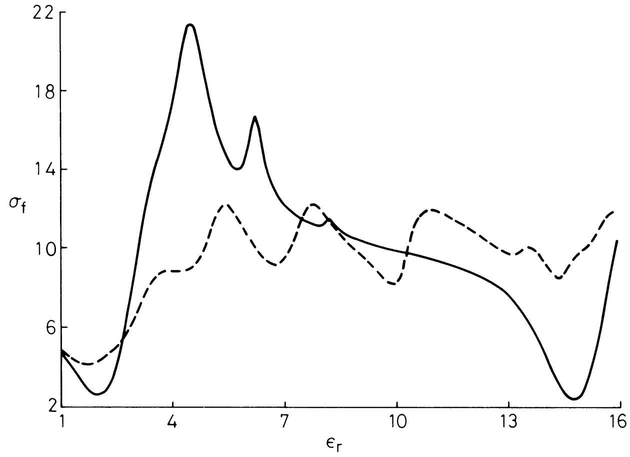

Fig. 8 *σ_f against ε_r with $\phi_0 = 180°$, $a = 0.3\lambda_0$, $b = 0.5\lambda_0$, $\eta_s = 0$ and $\varepsilon_{r1} = \varepsilon_r - j0.16$ (TM polarisation)*
——— $e = 0$
- - - - $e = 0.2\lambda_0$

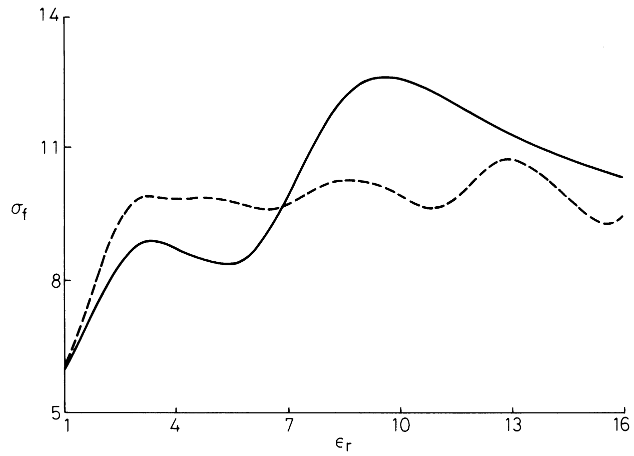

Fig. 9 *σ_f against ε_r with $\phi_0 = 180°$, $a = 0.3\lambda_0$, $b = 0.5\lambda_0$, $\eta_s = 0.5 - j0.5$ and $\varepsilon_{r1} = \varepsilon_r - j0.16$ (TM polarisation)*
——— $e = 0$
- - - - $e = 0.2\lambda_0$

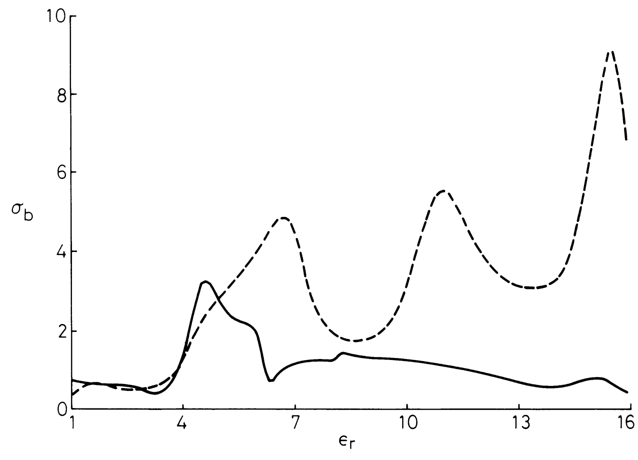

Fig. 10 *σ_b against ε_r with $\phi_0 = 180°$, $a = 0.3\lambda_0$, $b = 0.5\lambda_0$, $\eta_s = 0$ and $\varepsilon_{r1} = \varepsilon_r - j0.16$ (TM polarisation)*
——— $e = 0$
- - - - $e = 0.2\lambda_0$

do not show any resonance behaviour for the composite cylinder. The examination of Figs. 10 and 11 indicates

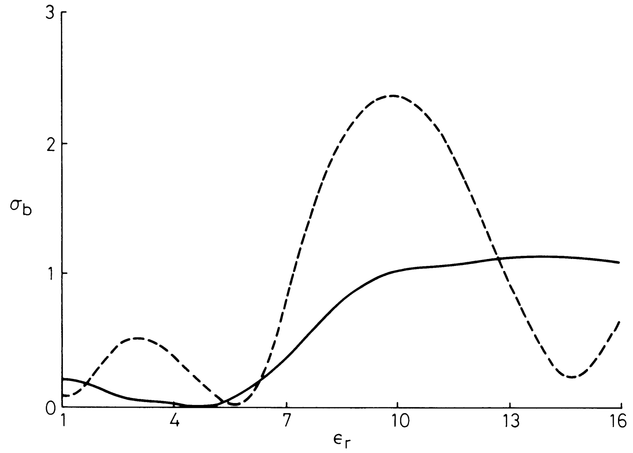

Fig. 11 *σ_b against ε_r with $\phi_0 = 180°$, $a = 0.3\lambda_0$, $b = 0.5\lambda_0$, $\eta_s = 0.5 - j0.5$ and $\varepsilon_{r1} = \varepsilon_r - j0.16$ (TM polarisation)*
——— $e = 0$ - - - - $e = 0.2\lambda_0$

that the offset parameter e significantly changes σ_b. For the case of an impedance core shown in Figs. 9 and 11, σ_f increases with no corresponding changes in σ_b as shown for $e = 0$ in the range $10 < \varepsilon_{r1} < 16$ and σ_b can be maximised with no significant change in σ_f as shown for $e = 0.2\lambda_0$.

Figs. 12 and 13 show σ_f and σ_b against e, respectively, due to a TM incident plane wave at $\phi_0 = 180°$ with $a =$

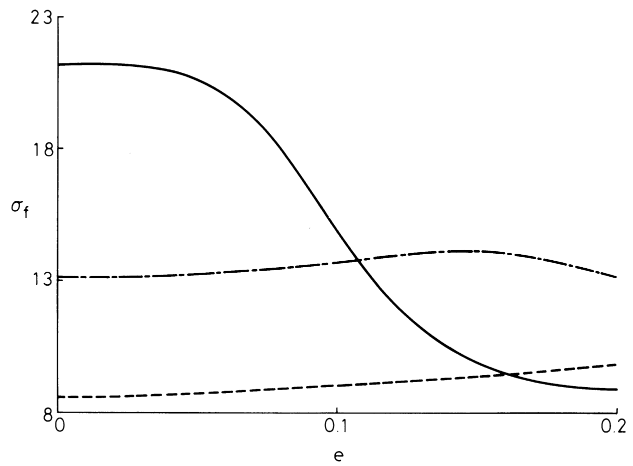

Fig. 12 *σ_f against e with $\phi_0 = 180°$, $a = 0.3\lambda_0$, $b = 0.5\lambda_0$, and $\varepsilon_{r1} = 4.37 - j0.16$ (TM polarisation)*
——— $\eta_s = 0$ —·— $\eta_s = 0.5 + j0.5$ - - - - $\eta_s = 0.5 - j0.5$

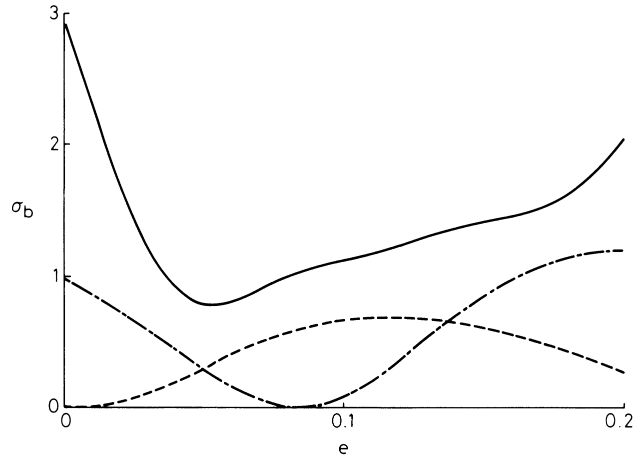

Fig. 13 *σ_b against e with $\phi_0 = 180°$, $a = 0.3\lambda_0$, $b = 0.5\lambda_0$, and $\varepsilon_{r1} = 4.37 - j0.16$ (TM polarisation)*
——— $\eta_s = 0$ —·— $\eta_s = 0.5 + j0.5$ - - - - $\eta_s = 0.5 - j0.5$

$0.3\lambda_0$, $b = 0.5\lambda_0$ and $\varepsilon_{r1} = 4.37 - j0.16$ for different values of η_s. These figures indicate that σ_f and σ_b are very sensitive for e variations when the core is perfectly conducting. However for an impedance core, it is possible to maximise or minimise σ_b without significant change in σ_f.

The near field components are also computed to investigate the effect of the parameters e and η_s. As an example, Figs. 14 and 15 are for the normalised electric field component due to a TM plane wave incident at an angle $\phi_0 = 180°$ with $a = 0.3\lambda_0$, $b = 0.5\lambda_0$ and $\varepsilon_{r1} = 4.37 - j0.16$. Fig. 14 is for a perfectly conducting core and Fig. 15 is for an impedance core where $\eta_s = 0.5 - j0.5$. It is obvious that the offset parameter e reduces the field values in the shadow region for both perfectly conducting and impedance cores whereas the capacitive core reduces the field values in all directions around the composite cylinder.

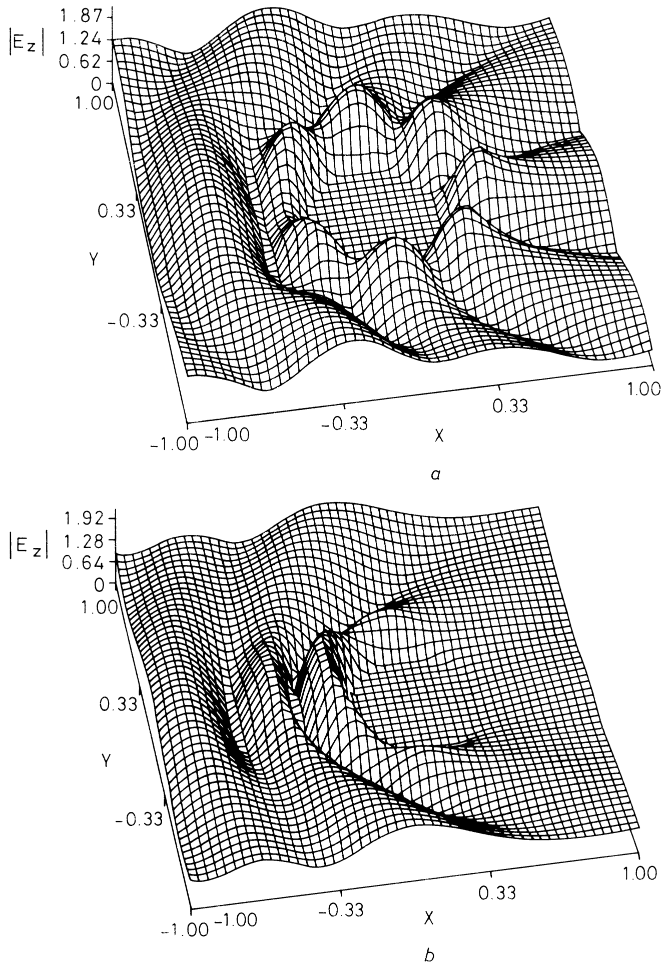

Fig. 14 *Normalised near electric field component with a perfectly conducting core for $\phi_0 = 180°$, $a = 0.3\lambda_0$, $b = 0.5\lambda_0$ and $\varepsilon_{r1} = 4.37 - j0.16$ (TM polarisation)*
a $e = 0$
b $e = 0.2\lambda_0$

4 Conclusion

This paper has given a rigorous analysis of the scattering from an impedance cylinder embedded eccentrically in a dielectric cylinder due to either a line source field or an incident plane wave. Both transverse electric and magnetic types of excitations are considered. The presented numerical results show the effect of different parameters on the scattering cross-section and how these parameters may be used to maximise or minimise the radar cross-section by proper selection of the electric and geometrical parameters. The generalisation of the present formulation to an arbitrary number of eccentric cylinders is currently being investigated by the authors. These geometries have useful biomedical applications as well as applications in the modelling of forests for remote sensing.

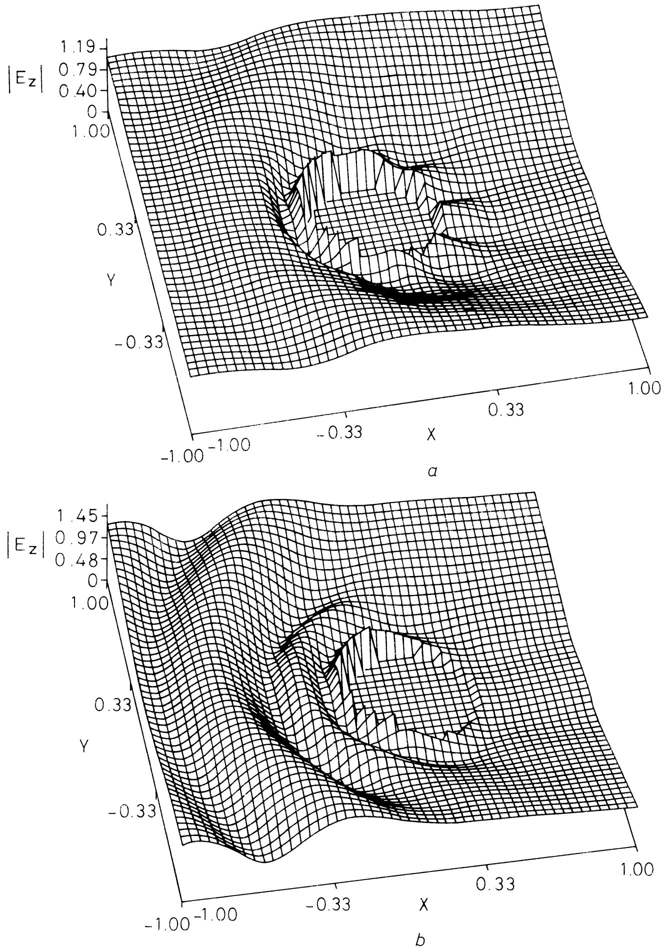

Fig. 15 *Normalised near electric field component with an impedance core for $\phi_0 = 180°$, $a = 0.3\lambda_0$, $b = 0.5\lambda_0$, $\varepsilon_{r1} = 4.37 - j0.16$ and $\eta_s = 0.5 - j0.5$ (TM polarisation)*
a $e = 0$
b $e = 0.2\lambda_0$

5 References

1 TANG, C.C.: 'Backscattering from dielectrically coated infinite cylindrical obstacles', *J. Appl. Phys.*, 1957, **28**, pp. 628–633
2 BHARTIA, P., SHAFAI, L., and HAMID, M.: 'Scattering by an imperfectly conducting cylinder with a radially inhomogeneous dielectric coating', *Int. J. of Electron.*, 1971, **31**, pp. 531–535
3 RAO, T.C., and HAMID, M.: 'Scattering by multi-layered dielectric-coated conducting cylinder', *Intl. J. Electron.*, 1975, **38**, pp. 667–673
4 ELSHERBENI, A.Z., and HAMID, M.: 'Scattering by a cylindrical dielectric shell with inhomogeneous permittivity profiles', *Intl. J. Electron.*, 1985, **58**, (6), pp. 559–562
5 ELSHERBENI, A.Z., RAGHEB, H.A., and HAMID, M.: 'Rigorous solution of the scattering by two multilayered dielectric cylinders'. IEEE/AP-S 1986, Symp., Philadelphia, PA, pp. 65–68
6 LEVIATAN, Y., BOAG, A., and BOAG, A.: 'Analysis of electromagnetic scattering from dielectrically coated conducting cylinders using a multifilament current model', *IEEE Trans.*, 1988, **AP-36,** pp. 1602–1607
7 KIM, H.T., and WANG, N.: 'UTD solutions for electromagnetic scattering by a circular cylinder with thin lossy coatings', *IEEE Trans.*, 1989, **AP-37**, pp. 1463–1472
8 WU, T.T., SHEN, L.C., and KING, R.W.P.: 'A dipole antenna with eccentric coating in a relatively dense medium', *IEEE Trans.*, 1975, **AP-23,** pp. 57–62
9 WU, T.K., and TSAI, L.L. 'Electromagnetic fields induced inside arbitrary cylinders of biological tissue', *IEEE Trans.*, 1977, **MTT-25,** pp. 61–56

10 GUY, A.W., CHOU, C., and LUK, K.: '915-MHz phased-array system for treating tumors in cylindrical structures', *IEEE Trans.*, 1986, **MTT-34,** pp. 502–507

11 ROUMELIOTIS, J.A., FIKIORIS, J.G., and GOUNARIS, G.P.: 'Electromagnetic scattering from an eccentrically coated infinite metallic cylinder', *J. Appl. Phys.*, 1980, **51,** (8), pp. 4488–4493

12 ROUMELIOTIS, J.A., and KOPIDIS, P.D.: 'Scattering of plane electromagnetic waves from an eccentrically coated infinite dielectric cylinder'. ICAP 83, 1983, pp. 186–188

13 ROUMELIOTIS, J.A., and FIKIORIS, J.G.: 'Scattering of plane waves from an eccentrically coated metallic sphere', *J. Franklin Institute*, 1981, **312,** pp. 41–59

14 VESELOV, G.I., and SEMENOV, S.G.: 'Theory of circular waveguide with eccentrically placed metallic conductor', *Radio Engg. and Electron. Phys.*, 1970, **15,** pp. 687–690

15 ROUMELIOTIS, J.A., and FIKIORIS, J.G.: 'Cutoff wavenumbers and the field of surface wave modes of an eccentric circular Goubau waveguide', *J. of Franklin Institute*, 1980, **309,** pp. 309–325

16 SENIOR, T.B.A.: 'Impedance boundary conditions for imperfectly conducting surfaces', *App. Sci. Rec.*, 1961, Section B, **8,** pp. 418–436

17 STRATTON, J.A.: 'Electromagnetic theory' (McGraw-Hill, New York, 1941)

18 HARRINGTON, R.: 'Time harmonic electromagnetic fields' (McGraw-Hill, New York, 1961)